P 6.19 DEVELOPING A CLIMATOLOGY OF CONVECTIVE PRECIPITATING PATTERNS IN AFRICA

Arlene G. Laing[1], Richard Carbone[1], Vincenzo Levizzani[2]

[1]National Center for Atmospheric Research, Boulder, CO, USA
[2]CNR-Institute of Atmospheric Sciences and Climate, Bologna, Italy

1. INTRODUCTION

The prediction of precipitation, particularly quantitative precipitation forecasting (QPF) remains one of the greatest problems in weather forecasting. Warm season precipitation presents an even greater challenge as the precipitation forms under relatively benign synoptic conditions and is strongly modulated by diurnal heating. The goal of this study is to investigate the propagation characteristics of convective precipitation in Africa. Here the term "warm season" as applied to Africa, a continent that straddles the equator, is more indicative of the precipitation regime change than the temperature.

In the United States (US), studies of the lifecycles of mesoscale convective systems (MCSs) have found that the majority of these systems initiate in the lee of the Rocky Mountains, move eastward and produce an overnight maximum in precipitation across the central plains, sometimes while undergoing various cycles of regeneration (Maddox 1980, Fritsch et al. 1986; Augustine and Caracena, 1994; Anderson and Arritt 1998, Trier et al. 2000). Using Weather Surveillance Radar-88 Doppler (WSR-88D) data, Carbone et al. (2002) found that clusters of heavy precipitation display coherent patterns of propagation across the continental US with phase speeds that exceed the speed of any individual MCS. Wang et al. (2004) created a similar climatology for the warm season in East Asia using infrared brightness temperatures from the Japanese Geostationary Meteorology Satellite (GMS). Their study showed propagation of cold-cloud clusters (or quasi-precipitation episodes) across zonal spans exceeding 2500km and duration greater than 45h when compared with 60h for the precipitation episodes in the US. The discovery of similar coherence is not surprising as MCSs in both regions have similar properties (Ma and Bosart 1987; Miller and Fritsch 1991).

Given the similarity in the properties of MCSs globally (Laing and Fritsch 1997), coherence in propagating characteristics is expected for precipitation over Africa. For example, the South Africa escarpment serves as the initiating point for convection that propagates to the east (Garstang et al. 1987; Laing and Fritsch 1993). In Sahelian Africa, the Jos Plateau (west Africa), the mountains of Dafur (western Sudan), and the Ethiopian highlands are regions where squall lines and mesoscale convective complexes originate (Tetzlaff and Peters 1988; Laing and Fritsch 1993). In Sahelian Africa, the Jos Plateau (west Africa), the mountains of Dafur (western Sudan), and the Ethiopian highlands are regions where squall lines and mesoscale convective complexes originate (Tetzlaff and Peters 1988; Laing and Fritsch 1993). Other studies of west African squall lines and cloud clusters have found that systems are modulated by easterly waves, the low-level jet, and moisture convergence in the lower troposphere (e.g., Payne and McGarry 1977; Frank 1978; Bolton 1984; Machado et al. 1993; Rowell and Milford 1993; Thorncroft and Haile 1995).

Convection and precipitation over Africa also varies inter-annually (Duvel 1989, Ba et al. 1995). Desbois et al. (1988) found that African squall lines had different initiation points, tracks, and speed for July 1983 and July 1985. Those differences are related to the large-scale dynamics such as variations in the migration of the Inter-tropical Convergence Zone.

2. DATA AND METHODS

The initial study period is May through August 1999. The primary data are digitized infrared (11.5μm) images from the European geostationary satellite (Meteosat). The images have a spatial resolution of 5km at the sub-point (0, 0) and are available at 30 minute intervals. Based on the prevailing low-level flow, the continental boundaries, and tracks of mesoscale convective systems, two domains will be studied (Fig. 1). The northern domain covers 5ºS to 25ºN and 20ºW to 40ºE from May to September. The southern domain is 35ºS to 5ºN and 5ºE to 40ºE from October to April includes prevailing easterlies north of 15ºS and prevailing westerlies south.

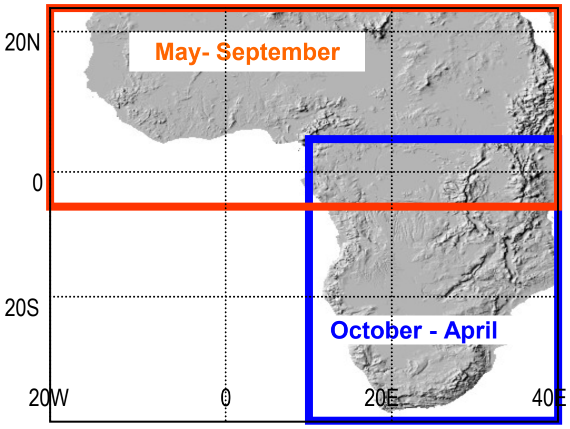

Fig. 1.Study domains overlaid on terrain map of Africa

Corresponding author address: Arlene Laing, NCAR/MMM, P.O. Box 3000, Boulder, CO, e-mail: laing@ucar.edu

A threshold brightness temperature is used to identify cold cloud systems that are most likely to be precipitating. Duvel (1989) used 253K as the threshold associated with convection while Arkin (1979) used 233K to identify accumulated convective precipitation. Like, Mathon and Laurent (2001), this study uses 213K to identify very deep convection over the Sahel. Further discrimination between precipitating and non-precipitating cold clouds is performed by comparing data from the Tropical Rainfall Measurement Mission (TRMM) Precipitation Radar and TRMM Microwave Imager. Consideration is also given to techniques for calibrating Meteosat IR with measurements from the Special Sensor Microwave Imager (SSM/I) (Levizzani et al. 1996). Corresponding water vapor images also help to distinguish between deep layer moisture of precipitating thunderstorms and layers of cirrus.

Satellite radiances and brightness temperatures are computed using a vicarious calibration method:

Radiance = Calibration factor (Count - Space Count)

where "Space Count" refers to the radiometer's offset for zero radiance (assumed to be the average count when the radiometer is viewing space).

For the range between 200K and 330K, radiance is converted to temperature using:

$$\textit{Radiance (T)} = e(A + \frac{B}{T})$$

where: radiance is in $Wm^{-2}\ sr^{-1}$, T is temperature (K), A is a regression coefficient (dimensionless), and B is a regression coefficient (K)

Propagation characteristics are determined using a methodology similar to that employed by Carbone et al. (2002) and Wang et al. (2004). Two-dimensional (2-D) arrays of temperature, latitude, and longitude are produced from a sub-sector of the full disc image. Every pixel colder than 213K constitutes an ‘‘event’’ at a given longitude–time coordinate. These pixels are accumulated and averaged hourly along each longitudinal grid (e.g., Fig. 2). A 2-D auto-correlation function is stepped through all points in the distance-time (Hovmoller) space and rotated until the correlation coefficient is maximized. Contiguous fits to the function define coherent patterns or “cloud streaks” (e.g., Fig 3). The zonal propagation speeds of the cloud streaks are computed from the slopes in Hovmoller space. The statistics of cloud streaks with durations greater than 3h are compared with the results of Carbone et al. (2002) and Wang et al. (2004).

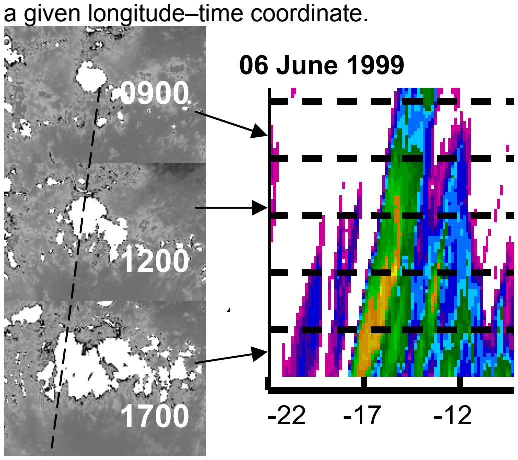

Fig. 2. Enhanced IR Images (white areas have Tb ≤ 213K) and associated cloud streaks in Hovmoller (longitude-time) space

Global Reanalysis data are used to analyze the large-scale environments associated with deep convective development. Reanalysis pressure level data have a 2.5 degree grid and are provided daily at 0000, 0600, 1200, and 1800UTC.

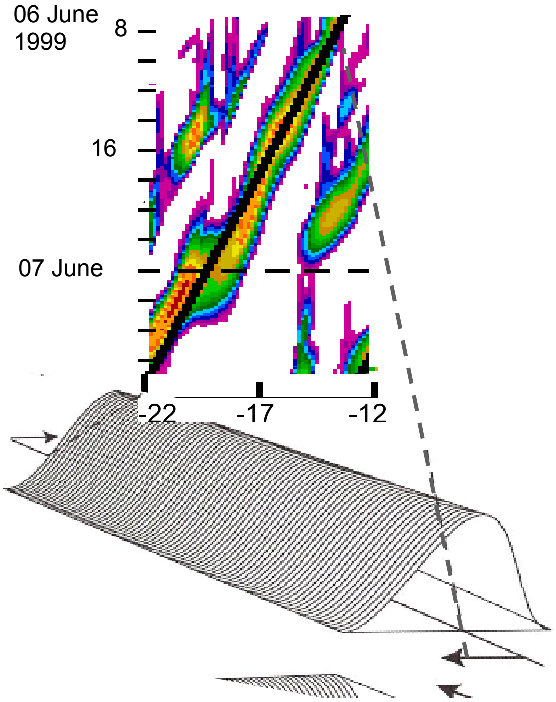

Fig. 3. Schematic of a Hovmoller diagram with a cloud streak and auto-correlation function. The straight black line is an example of a “fit” where the function matched well with the cold cloud top temperatures.

4. Convective cloud streak patterns

Deep convection in Africa exhibited coherent patterns and propagating characteristics similar to North America and East Asia except for westward propagation. Examples of cloud streaks for each month are shown in Fig 4.

Convection was most frequently initiated west of Ethiopian Highlands (west of 35ºE) during all months. Frequent initiation of convection also occurs in the lee of the Dafur mountains (west of 20ºE), Jos Plateau and Cameroon Mountains (west of 10ºE), as well as along the western coast of the Sahel.

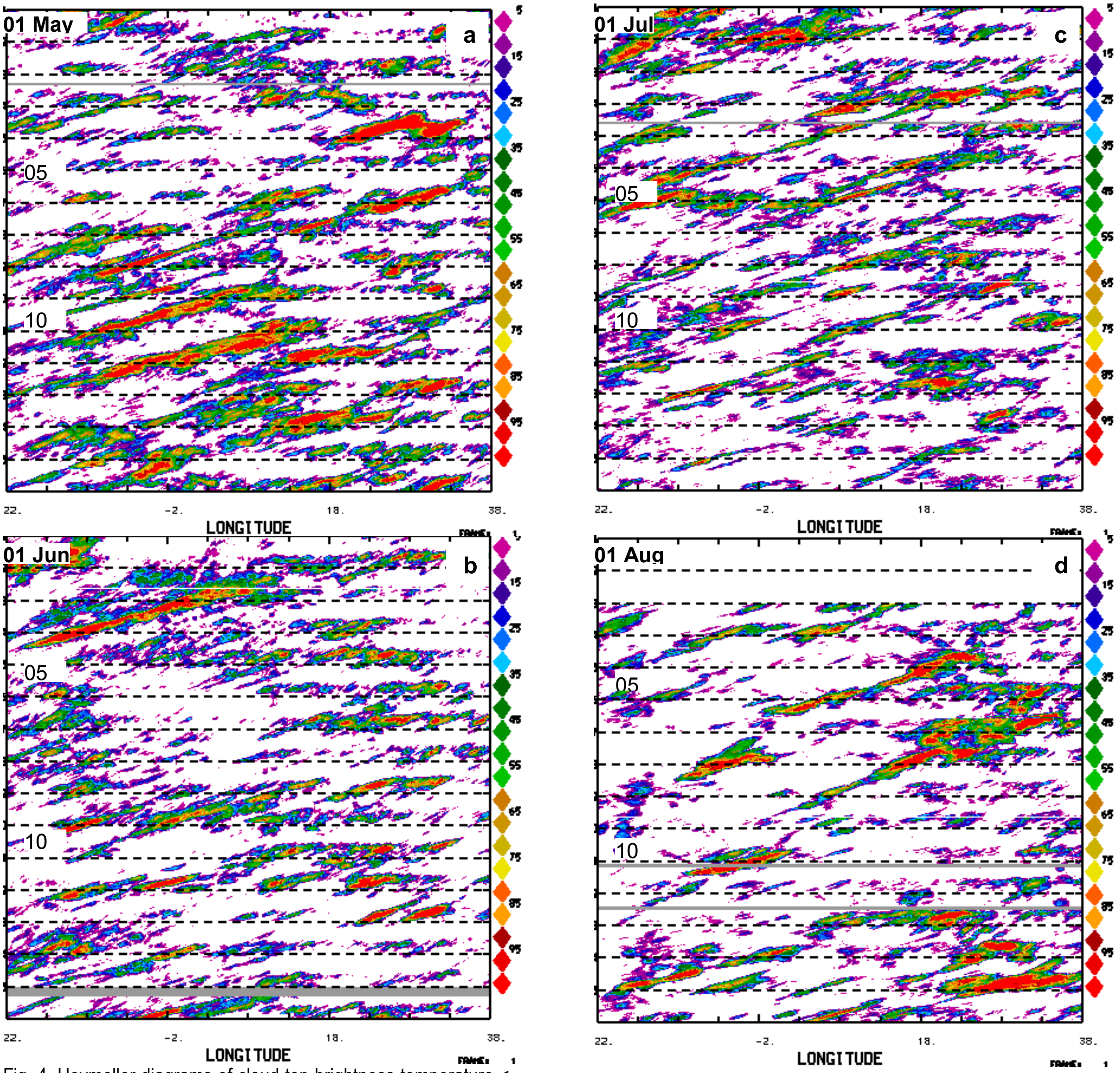

Fig. 4. Hovmoller diagrams of cloud top brightness temperature < 213K for the period of (a) 1-15 May, (b) 1-15 June, (c) 1-15 July, and (d), 1-15 August of 1999.

4.1 Span, duration, and speed

The mean zonal span and duration for the four month period, May to August 1999, were 847km and 17.9h. A few episodes spanned 4000km and lasted longer than 80h (Fig. 5). It should be noted that the longitudinal domain for Africa was 60degrees compared with 50 and 37 degrees for East Asia and the US, respectively. Having a larger domain allowed cloud streaks to be tracked over a greater distance and through a greater number of diurnal cycles. The phase speeds for most convective cloud streaks were 10 - 20 ms^{-1} with an overall mean of 13.5 ms^{-1} (Fig. 6), which is similar to the US and East Asia (Table 1).

Table 1. Cold cloud streak statistics for the US, East Asia, and Africa.

Region (Domain Longitude)	Span (km)	Duration (h)	Speed (ms^{-1})
Contiguous US (37deg)	1 per day mean - 838	1 per day mean – 18.5	Mean – 12.6
East Asia (50deg)	1 per day mean - 620	1 per day mean 11.6h	Mean – 12.4
Africa (60deg)	Overall Mean - 874	Overall mean – 17.9	Mean – 13.5

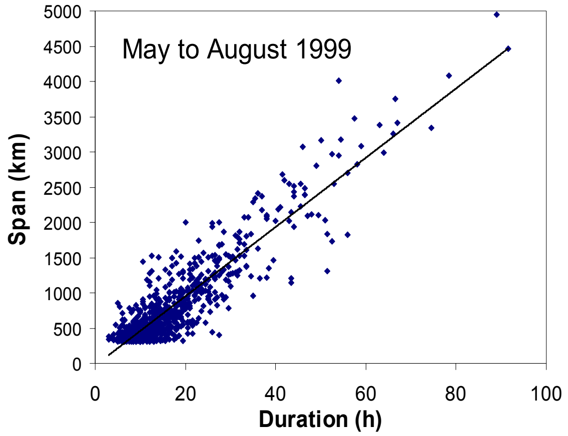

Fig. 5. Scatter plot of zonal span versus duration of all convective episodes or "streaks" for May to August 1999.

4.2 Diurnal Cycle

The mean diurnal cycle was determined by computing the occurrence of precipitating convection at a particular longitude at the same time of day. For the region east of 30ºE, most of the convection occurred in the afternoon. The formation of convection over the eastern portion of the domain is consistent with the principles of thermal heating of elevated terrain and studies cited in Section 1.

Farther west, maxima can be found in the late evening to nighttime hours. The diurnal cycle of convection varies longitudinally and temporally (Fig 7). For instance, convection in late June (Fig 7b) and early July (not shown) exhibited four diurnal cycles. The pattern indicates late evening and nighttime maxima and regeneration of convection. In contrast, early May (Fig 7a) had mostly afternoon convection (diurnal maximum).

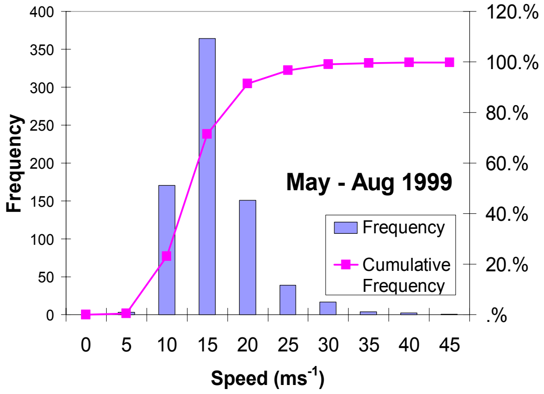

Fig. 6. Frequency and Cumulative Frequency of the phase speed of all cloud streaks for May to Aug 1999.

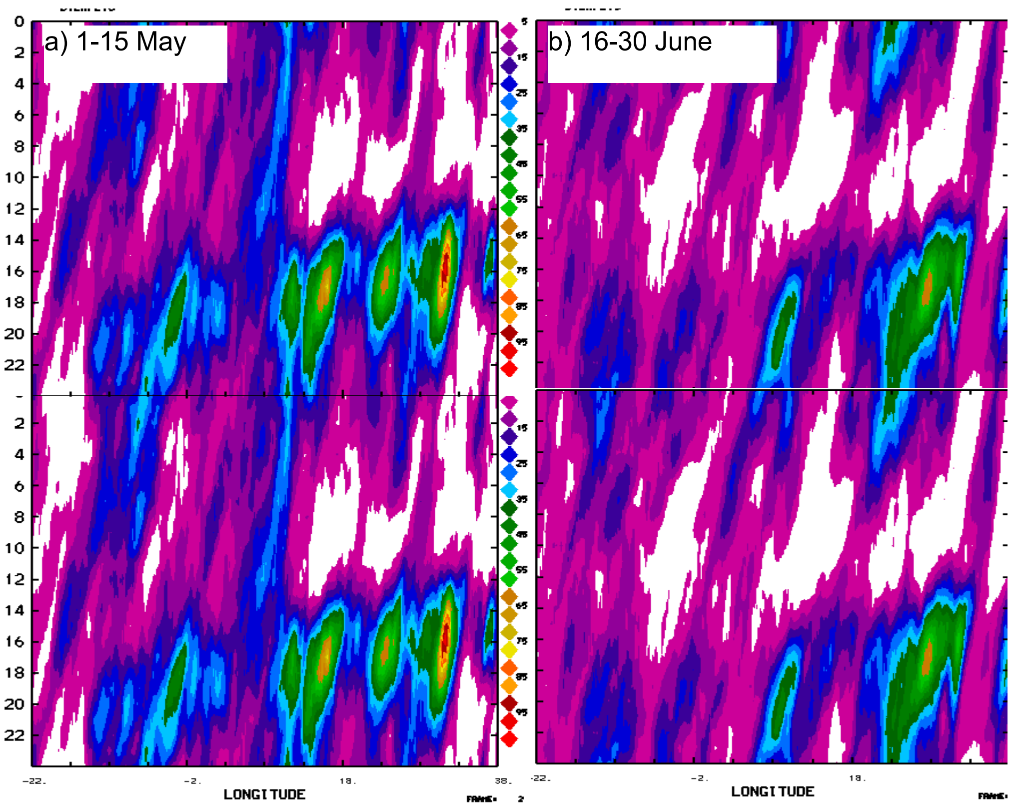

Fig. 7. Mean diurnal cycle for (a) 1-15 May, (b) 16-30 June 1999. Times are UTC

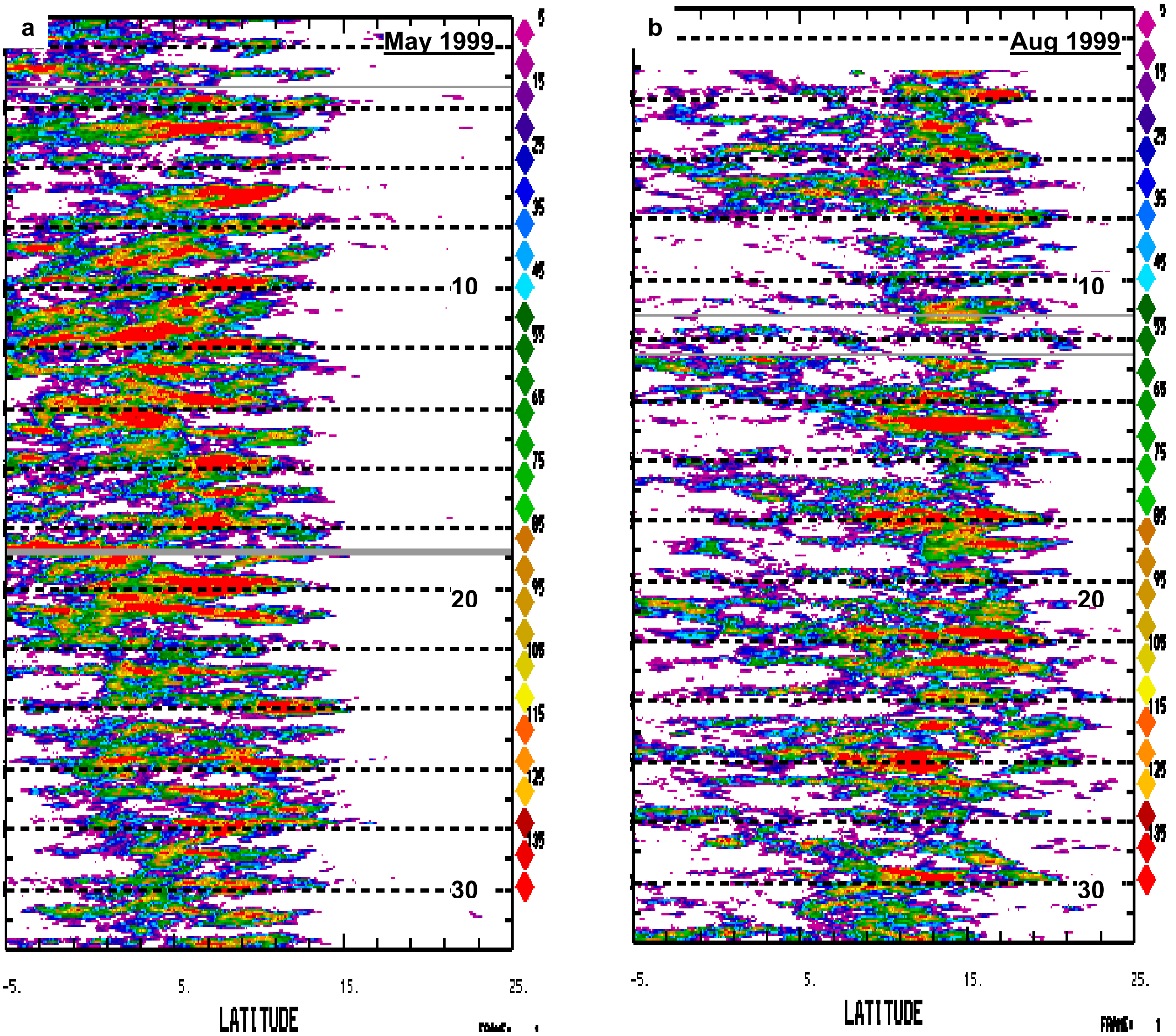

Fig. 8. Hovmoller (latitude – time) diagrams of cloud top brightness temperature < 213K for the period of (a) 1-31 May and (b) 1-31 August of 1999.

4.3 Meridional propagation

Cold cloud streaks display very little propagation in the meridional direction (Fig. 8). However, the latitudinal belt of convection and precipitation migrates northward with the solar cycle and the ITCZ. During May, deep convection occurs mostly south of 15ºN. By August, most deep convection develops between 8ºN and 20ºN although some deep convection occurs south of the equator. The development of convection is also tied to the low-level African easterly jet that becomes firmly established as the season progresses.

5. Concluding Remarks

Preliminary results of a multi-year study of precipitating convection in Africa were presented. It was found that deep convection in Africa displays patterns of coherence that are similar to those observed from radar-based studies in the US and infrared satellite- based studies in East Asia. For the three regions, most cold cloud streaks had phase speeds between 10 and 20 ms-1. Longer-lived streaks were observed in Africa, where the longitudinal extent of the study domain was almost twice the length of the US domain used by Carbone et al. (2002).

Most convection within the study domain initiated west of the Ethiopian Highlands with secondary maxima influenced by the Dafur Mountains, and higher terrain along the west coast of Africa.

In further study, additional years will be analyzed and the large-scale environment will be examined to determine the primary steering level for the cold cloud streaks.

Acknowledgements

This research is sponsored by National Science Foundation support to the U.S. Weather Research Program. Satellite data were provided by EUMETSAT archives. Thanks to Sherrie Frederick and John Tuttle for assistance with data processing and to Chris Davis for advice.

REFERENCES

Augustine, J. A. and F. Caracena, 1994: Lower-tropospheric precursors to nocturnal MCS development over the Central United States. *Wea. Forecasting*, **9**, 116-135.

Anderson, C. and R. Arritt, 1998: Mesoscale convective complexes and persistent elongated convective systems over the United States during 1992 and 1993. *Mon. Wea. Rev.*, **126,** 578-599.

Arkin, P.A., The relationship between fractional coverage of high cloud and rainfall accumulation during GATE over the B-scale array. *Mon. Wea. Rev.*, **107**, 1382-1387.

Ba, M. B., R. Frouin, S.E. Nicholson, 1995: Satellite-derived inter-annual variability of west African rainfall during 1983–88. . *J. Appl. Meteor*, 34, 411–431.

Bolton, D. A., 1984: Generation and propagation of African squall lines. *Quart. J. Roy. Meteor. Soc.*, **110**, 695-721.

Carbone, R.E., J.D. Tuttle, D. Ahijevych, S.B. Trier, 2002: Inferences of predictability associated with warm season precipitation episodes, *J. Atmos. Sci.*, **59**, 2033-2056.

Desbois, M., T. Kayiranga, B. Gnamien, S. Guessous, and L. Picon, 1988: Characterization of some elements of the Sahelian climate and their annual variations for July 1983, 1984, and 1985 from the analysis of Meteosat ISCCP data. *J. Climate.*, **9**, 867-904.

Duvel, J-. P., 1989: Convection over tropical Africa and the Atlantic ocean during northern summer. Part I: Interannual and diurnal variations. *Mon. Wea. Rev.*, **117**, 2782-2799.

Frank, W. M., 1978: The life cycles of GATE convective systems. *J. Atmos. Sci.*, **35**, 1256-1264.

Fritsch, J. M., R. J. Kane and C. H. Chelius, 1986: The contribution of mesoscale convective weather systems to the warm season precipitation in the United States., *J. Clim.Appl.Meteo.*, **25**, 1333-1345.

Garstang, M., B. E. Kelbe, G. D. Emmitt, W. B. London, 1987: Generation of convective storms over the escarpment of northeastern South Africa. *Mon. Wea. Rev.*, **115**, 429-443.

Laing, A. G. and J. M. Fritsch, 1993: Mesoscale convective complexes in Africa. *Mon. Wea. Rev.*, **121**, 2254-2263.

Laing, A.G. and J.M. Fritsch, 1997: The global population of mesoscale convective complexes. *Quart. J. Roy. Meteor. Soc.,* Jan B, **123**, 389-405.

Levizzani, V., F. Porcu, F. S. Marzano, A. Mugnai, E. A. Smith, F. Prodi, 1996: Investigating a SSM/I microwave algorithm to calibrate METEOSAT infrared instantaneous rain rate estimates. *Meteor. Appl.*, **3**, 5-17.

Ma, K-Y. and L. F. Bosart, 1987: A synoptic overview of a heavy rain event in Southern China. *Wea. Forecasting,* **2**, 89-112.

Machado, L. A. T., J.-Ph. Duvel, and M. Desbois, 1993: Diurnal variations and modulations by easterly waves of the size distribution of convective cloud clusters over West Africa and the Atlantic Ocean. *Mon. Wea. Rev.*, **121**, 37-49.

Mathon, V. and H. Laurent, 2001: Lifecycle of Sahelian mesocale convective cloud systems. *Q.J.R. Meteorol. Soc.*,**127**, 377-406.

Miller, D. and J.M. Fritsch, 1991: Mesoscale convective complexes in the western Pacific region. *Mon. Wea. Rev.*, **119**, 2978-2992.

Payne, S. W. and M. M. McGarry, 1977: The relationship of satellite inferred convective activity to easterly wave over west Africa and the adjacent ocean during Phase III of GATE., *Mon. Wea Rev.*, **105**, 413-420.

Rowell, D. P. and J. R. Milford, 1993: On the generation of African squall lines. *J. Climate,* **6**, 1181-1193.

Tetzlaff, G. and M. Peters, 1988: A composite study of early summer squall lines and their environment over West Africa. *Meteorol. Atmos. Phys.*, **38**, 153-163.

Thorncroft, C. D. and M. Haile, 1995: The mean dynamic and thermodynamic fields for July 1989 over Tropical North Africa and their relationship to convective storm activity. *Mon. Wea. Rev.*, **123**, 3016-3031.

Trier, S. B., C. A. Davis, and J. D. Tuttle, 2000: Long-Lived Mesoconvective Vortices and Their Environment. Part I: Observations from the Central United States during the 1998 Warm Season. *Mon. Wea. Rev.*, **128**, 3376-3395.

Wang, C-C, G. T-J. Chen, R. E. Carbone, 2004: A climatology of warm season cloud patterns over East Asia based on GMS Infrared Brightness Temperature Observations. *Mon Wea. Rev.*, 1606–1629.